UC Irvine
Faculty Publications

Title
Forcing of the wintertime atmospheric circulation by the multidecadal fluctuations of the North Atlantic ocean.

Permalink
https://escholarship.org/uc/item/11n2t8n4

Journal
Environmental Research Letters, 9(3)

Authors
Magnusdottir, G
Peings, Y

Publication Date
2014-04-01

Supplemental Material
https://escholarship.org/uc/item/11n2t8n4#supplemental

Copyright Information

Peer reviewed

Forcing of the wintertime atmospheric circulation by the multidecadal fluctuations of the North Atlantic ocean

Forcing of the wintertime atmospheric circulation by the multidecadal fluctuations of the North Atlantic ocean

Yannick Peings and Gudrun Magnusdottir

Department of Earth System Science, University of California, Croull Hall, Irvine, CA 92697-3100, USA

E-mail: ypeings@uci.edu

Abstract

The North Atlantic sea surface temperature exhibits fluctuations on the multidecadal time scale, a phenomenon known as the Atlantic Multidecadal Oscillation (AMO). This letter demonstrates that the multidecadal fluctuations of the wintertime North Atlantic Oscillation (NAO) are tied to the AMO, with an opposite-signed relationship between the polarities of the AMO and the NAO. Our statistical analyses suggest that the AMO signal precedes the NAO by 10–15 years with an interesting predictability window for decadal forecasting. The AMO footprint is also detected in the multidecadal variability of the intraseasonal weather regimes of the North Atlantic sector. This observational evidence is robust over the entire 20th century and it is supported by numerical experiments with an atmospheric global climate model. The simulations suggest that the AMO-related SST anomalies induce the atmospheric anomalies by shifting the atmospheric baroclinic zone over the North Atlantic basin. As in observations, the positive phase of the AMO results in more frequent negative NAO—and blocking episodes in winter that promote the occurrence of cold extreme temperatures over the eastern United States and Europe. Thus, it is plausible that the AMO plays a role in the recent resurgence of severe winter weather in these regions and that wintertime cold extremes will be promoted as long as the AMO remains positive.

S Online supplementary data available from stacks.iop.org/ERL/9/034018/mmedia

1. Introduction

While the positive phase of the North Atlantic Oscillation (NAO) prevailed during the 1980s and 1990s (Hurrell *et al* 2003), negative values of the NAO index (also depicted through the Northern Annular Mode, NAM, index) have been observed during recent winters (Cohen *et al* 2012). During the negative NAO, the North Atlantic jet stream and storm track are shifted southwards, leading to more intense cold-air outbreaks over northern Europe and the eastern United States. In association with this recent trend of the NAO/NAM, cold temperatures and increased snowfall were observed over large areas of North America, Europe and Asia, especially during the 2009–2010, 2011–2012 and 2012–2013 winters (Cattiaux *et al* 2010, Coumou and Rahmstorf 2012). Meanwhile, the Arctic has warmed more rapidly than other regions of the globe due to several positive feedback mechanisms that amplify both the surface warming (a phenomenon referred to as the Arctic amplification (e.g. Screen and Simmonds 2010)) and the decline of sea ice extent (Stroeve *et al* 2012). Some

studies suggest that the Arctic amplification has favored the occurrence of the cold extreme events that have been observed over continental regions of the Northern hemisphere (NH) mid-latitudes in recent winters (Tang *et al* 2013, Francis and Vavrus 2012). According to this hypothesis, the Arctic amplification reduces the temperature gradient between the polar region and the mid-latitudes, resulting in a meridional elongation and a slow-down of the planetary waves. Atmospheric blocking and southward advection of Arctic air masses become more frequent, leading to an increase of extreme weather events in mid-latitudes. However, such an atmospheric response to the present warming of the Arctic is still hardly detectable in observations (Screen and Simmonds 2013, Barnes 2013) and it is weak in experiments performed with an atmospheric global climate model (GCM) that is forced with the recent Arctic sea ice concentration (Peings and Magnusdottir 2014).

Another potential driver of these recent climatic anomalies is the Atlantic Multidecadal Oscillation (AMO). The AMO consists of an alternation between warm and cold sea surface temperature (SST) anomalies in the North Atlantic basin, with a period of ~60–70 years (Kerr 2000). The AMO is visible in SST measurements that go back to the 19th century as well as in paleoclimatic reconstructions (Knudsen *et al* 2011). Given the long periodicity of the AMO, *in situ* SST observations are not sufficient to determine whether this mode is a long-lived natural oscillation or simply represents some particular fluctuations over the recent time period. However, control simulations with coupled ocean–atmosphere GCMs suggest that AMO-like fluctuations are closely tied to the variability of the Atlantic Meridional Overturning Circulation (AMOC) (Wang and Zhang 2013). Observational analyses support the thesis that the AMO is a natural process related to the adjustment of the thermohaline circulation to sea ice and freshwater export from Arctic (Dima and Lohmann 2007). This point is still a matter of debate and other authors propose that the multidecadal fluctuations of North Atlantic SST may be externally forced, in particular by the anthropogenic emissions of greenhouses gases (GHG) and/or aerosols (Booth *et al* 2012).

Regardless of the origins of the AMO, its fluctuations are associated with numerous climatic phenomena (Knight *et al* 2006), especially in summer. Fewer studies have investigated the wintertime atmospheric response to AMO forcing. However, new findings suggest that the AMO induces NAO-like anomalies of opposite polarity in winter (Gastineau *et al* 2013, Kavvada *et al* 2013, Msadek *et al* 2011), and that the positive AMO increases the likelihood of blocking of the atmospheric circulation over the North Atlantic (Häkkinen *et al* 2011). This is consistent with the occurrence of recent severe winters as the AMO shifted from the negative to the positive polarity around the end of the 1990s. The AMO has the potential to drive the atmospheric circulation through sea surface temperature (SST) anomalies, but also through associated changes in Arctic sea ice. Indeed, the AMOC/AMO cycles are associated with sea ice concentration (SIC) anomalies in the North Atlantic/Arctic basin (Mahajan *et al* 2011). Some of the recent winter climate anomalies that have been attributed to sea ice loss (and indirectly to global change) may therefore have been related to natural variability of the AMOC/AMO. In the present letter,

we aim to determine whether the AMO may have played a role in the severity of winters observed over the NH mid-latitudes these last years. We consider the impacts of the AMO on the multidecadal fluctuations of seasonal and intraseasonal atmospheric processes by combining observational/reanalysis data and numerical experiments using an atmospheric GCM.

2. Methods

2.1. AMO and NAO indices

A wintertime AMO index is constructed over the 1870–2012 period using the HadISST dataset (Rayner *et al* 2003). The monthly SST anomalies are determined with respect to the 1981–2010 climatology, then the winter AMO index is computed by averaging the monthly SST anomalies over the North Atlantic [75W/5W; 0/70N] from December to March (DJFM). The global anomalies of SST are subtracted in order to remove the global warming trend and the tropical oceans influence, as suggested by Trenberth and Shea (2006). A Lanczos low-pass filter is applied to the time series to remove the high-frequency variability (21 total weights and a threshold of 10 years, with the end points reflected to avoid losing data). Due to the use of the revised AMO index (method of Trenberth and Shea 2006) instead of the original index (based on a linear detrending of North Atlantic SST anomalies, used for example in Knight *et al* 2006), the AMO index exhibits little fluctuations prior to the 1930s (figure 1(a)). This difference between the revised and original AMO index is somewhat uncertain given the poor coverage of SST observations in the early period (that is critical for the revised AMO index because global SST anomalies are subtracted). We decided to adopt the revised AMO index of Trenberth and Shea (2006) since it isolates the Atlantic variability from global warming and tropical influences. Our results are not sensitive to the exact choice of the AMO index as the analyses are conducted over the 1901–2010 period and for most of that period there is good agreement between the two indices.

A decadal NAO index is computed from the 20th century reanalysis (20CR), which is available over 1871–2010 and is based on the assimilation of surface pressure observations only (Compo *et al* 2011). We use the station-based formulation based on the Stykkisholmur/Reykjavik and Lisbon anomalous sea-level pressure (SLP) difference (Hurrell *et al* 2003). The high-frequency fluctuations are removed from the NAO index using the same Lanczos filter as for the AMO index. Two alternative indices of the decadal NAO are also used to assess the dependence of the results on the choice of the NAO index: the EOF-based NAO index (1st EOF of SLP over the North Atlantic region [20N/85N-75W/20E]) and the Hurrell DJFM NAO index available on https://climatedataguide.ucar.edu/climate-data/hurrell-north-atlantic-oscillation-nao-index-station-based. The latter index is constructed using station measurements and is therefore not affected by any assimilation process, unlike 20CR.

2.2. Numerical simulations

We use the latest version of the Community Atmospheric Model (CAM5) to determine the response of the wintertime atmospheric circulation to the AMO forcing. Two 50-year
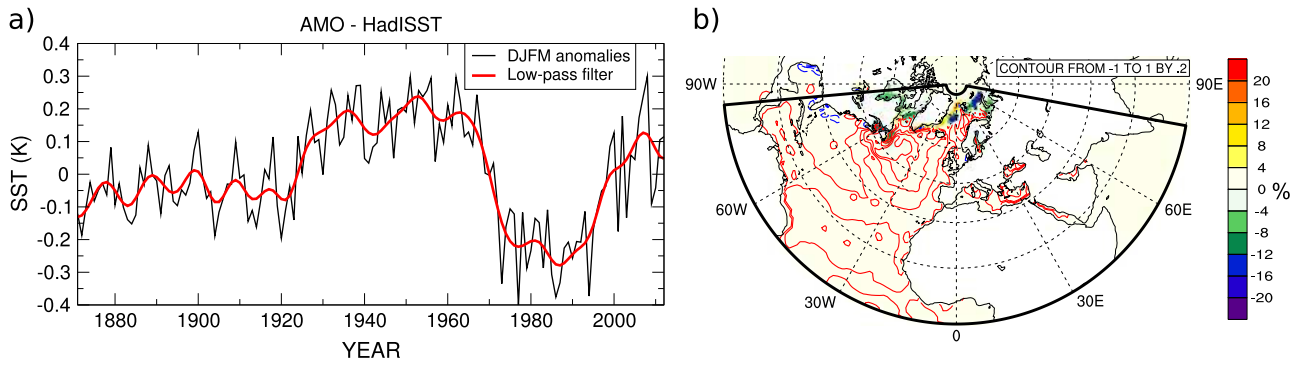
Figure 1. AMO signature in the observations. (a) Winter (DJFM) AMO time series from the HadISST dataset (red). Seasonal anomalies are shown in black. (b) SST (contours in K, positive contours in red, negative contours in blue) and SIC anomalies (shading in %) associated with the AMO signal in observations over 1951–2012 (difference between positive and negative phases of the AMO, based on composite analysis to select positive and negative AMO years). The domain on which the AMO anomalies are imposed in the model is also shown.

simulations are performed with a prescribed and constant annual cycle of SST and SIC, representative of the 1979–2000 climatology except over the North Atlantic. The GHG/aerosols concentrations are representative of the year 2000. The two experiments only differ by the prescribed SST/SIC in the North Atlantic region (see figure 1(b) for the domain and the perturbation corresponding to the AMO). In the first simulation (AMOp), the annual cycle of the SST/SIC anomalies representative of the positive AMO cycle is superimposed on the 1979–2000 climatological SST/SIC over the North Atlantic. In the second simulation (AMOn), the annual cycle of SST/SIC anomalies that is superimposed is representative of the negative AMO cycle. The SST/SIC anomalies that are prescribed to the model (figure 1(b)) come from a composite analysis of the HadISST observations based on the value of the AMO index over 1951–2012 (the DJFM-mean AMO value must be greater/lower than the upper/lower quartile of the distribution). The 1951–2012 years have been selected because of the higher reliability of the SIC data on this period. Starting in 1978, SIC in HadISST is estimated from satellite observations while prior to 1978 SIC is reconstructed from different sources of data that comprise observations of the marginal ice zone over North Atlantic from the 1950s (Walsh and Chapman 2001). The anomalies are detrended and low-pass-filtered before computing the composites in order to isolate the decadal fluctuations of SST and SIC that are associated with the AMO. These simulations give us a sample of 50 winters for each polarity of the AMO with exactly the same forcing of SST and SIC. 50-year winter means of the two simulations are then subtracted to assess the atmospheric response to the AMO forcing.

2.3. Statistical methods

The North Atlantic weather regimes are computed using a *k*-mean clustering algorithm applied to the daily anomalies of the 500 hPa geopotential height (Z500), both for 20CR and the CAM5 simulations. The daily anomalies are with respect to the 1981–2010 climatology in 20CR (50-year mean climatology in CAM5) and are computed over the [80W/30E; 20/80N] domain. Each day is attributed to one

of the four centroids of the *k*-mean partition according to a spatial correlation criterion ($r > 0.25$ between the anomaly and the centroid). One regime must last at least 3 days to be selected as a regime occurrence. The transient eddy activity is defined as the standard deviation of the daily bandpass-filtered (between 2 and 6 days) Z500. The statistical significance of the anomalies is determined in 20CR and in the CAM5 simulations using a two-sided Student *t*-test (considering each seasonal value as independent). The cold spell days are defined in agreement with the recommendation of the World Meteorological Organization (WMO). At each grid point, a cold spell is identified when the surface temperature is below the 10th percentile of the corresponding day for at least six consecutive days.

3. Result

3.1. Link between the multidecadal variations of the NAO and of the AMO

Figure 1(a) shows the winter-mean AMO index computed over 1870–2012. The AMO alternates between warm and cold SST anomalies over the North Atlantic basin and is also associated with SIC anomalies in the Atlantic subpolar region. During the positive AMO, the SST is warmer than during the negative AMO, with a maximum amplitude off the coast of Newfoundland (up to ∼+1.5 °C) and less sea ice in the high latitudes (figure 1(b)).

The NH atmospheric circulation that is associated with the AMO fluctuations in the observations is determined by computing composites of the detrended SLP of 20CR. The 1901–2010 period is retained for this computation since both SST and SLP data are less certain prior to this date. That also gives us two samples of sufficient and consistent size for each phase of the AMO. Based on the values of the AMO index (figure 1(a)), the years 1925–1969 and 1999–2010 are considered positive AMO years (57 years AMO+), while the years 1901–1924 and 1970–1998 are considered negative AMO years (53 years AMO−). The difference in winter SLP between the AMO+ and AMO− years is depicted in figure 2(a) (shading) for the Northern Hemisphere. For comparison, the NAM pattern is also shown (1st EOF mode
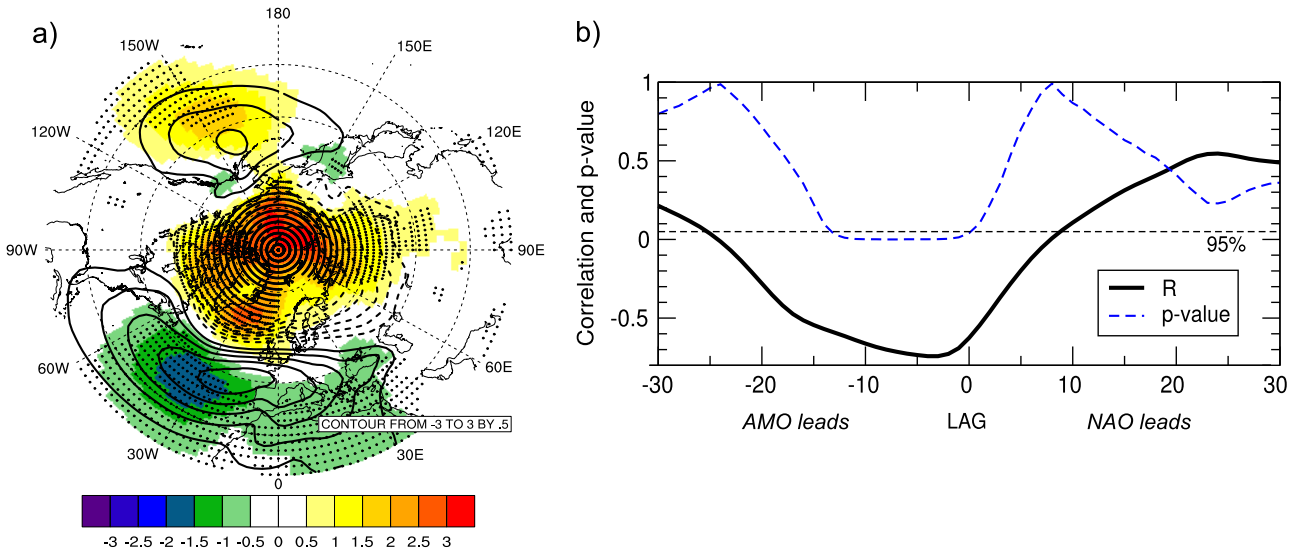
Figure 2. Relationship between the AMO and the winter NAO. (a) Winter (DJFM) SLP anomalies associated with the AMO signal (57 AMO+ years minus 53 AMO− years, see list of years in text) in 20CR over 1901–2010 (shading in hPa). The Northern Annular Mode pattern computed from an EOF analysis using the 20CR SLP is shown in contours (hPa). Anomalies significant at the 95% level are stippled. (b) Lead–lag correlations (black curve) between the DJFM AMO and the DJFM decadal NAO indices over 1901–2010. The statistical significance of the correlation is depicted by the *p*-value (blue dashed curve), computed using a bootstrap method that takes into account autocorrelations in the time series. The 95% confidence level is indicated by the dashed black line.

of SLP north of 20°N). The SLP anomaly that is associated with the AMO signal is reminiscent of the NAO (spatial correlation of −0.9 with the NAM pattern over the North Atlantic sector). The AMO+ is associated with the NAO−, the AMO− with NAO+. This result is robust across the multidecadal sub-intervals corresponding to the AMO+ and AMO− phases (figure S1 available at stacks.iop.org/ERL/9/034018/mmedia), except for the most recent time interval (1999–2010), which is too short for robust conclusions. The 1871–1900 time interval is also shown for comparison, but data for that time interval (both SST and SLP) are less certain. The amplitude of the SLP signal (figure 2(a) for the entire winter) is stronger in late winter (February–March) compared to early winter (December–January) as illustrated in figure S2 (available at stacks.iop.org/ERL/9/034018/mmedia).

In order to further investigate the multidecadal relationship that exists between the winter AMO index and the NAO, a decadal winter NAO index is constructed using the 20CR SLP (see section 2.1). The decadal NAO index is shown in figure S3 (available at stacks.iop.org/ERL/9/034018/mmedia) along with the AMO index. The correlation between the indices is −0.52 over 1871–2010, and −0.64 over 1901–2010. Both correlations are statistically significant at the 95% confidence level (the important autocorrelation of the time series due to their low-frequency spectrum is considered in the statistical test through a bootstrap procedure). The negative correlation is not only synchronous but is also significant, and even larger, when the AMO leads the NAO by up to 10–15 years (figure 2(b)). This suggests that the AMO is a source of predictability for the multidecadal fluctuations of the NAO, with a lag that is particularly relevant for decadal forecasting. The lead/lag correlations shift from negative values towards positive values when the NAO leads the AMO, reflecting the

approximately 60-yr cycle of the AMO and a possible response of the AMO to the NAO (Li *et al* 2013). The AMO–NAO relationship is independent of the choice of method and dataset for computing the NAO index (figure S4 available at stacks. iop.org/ERL/9/034018/mmedia).

3.2. Signature of the AMO in multidecadal fluctuations of intraseasonal weather regimes

The AMO footprint is also found in multidecadal fluctuations of intraseasonal weather phenomena such as atmospheric blocking (Häkkinen *et al* 2011). We investigate the intraseasonal response of the wintertime atmospheric circulation to the AMO by examining the North Atlantic weather regimes in 20CR. The daily Z500 is classified with a clustering algorithm (see section 2.3). The four weather regimes typically found over the North Atlantic in winter are identified in figures 3(a)–(d). They are: the blocking regime, the Atlantic Ridge regime, the positive NAO regime (NAO+, also called the Atlantic low regime) and the negative NAO regime (NAO−) (Cassou 2008). Each weather regime is associated with different climatic conditions over Europe and North America. In particular, the negative NAO and the blocking regimes are generally associated with cold extreme temperatures over Europe and the eastern United States (US) (Yiou and Nogaj 2004). The distributions of frequencies of the regimes are extracted for each winter of the 1901–2010 period. The regime frequencies of 20CR compare well with other reanalysis products over the periods of overlap (Ouzeau *et al* 2011) and are expected to be reliable for the earlier part of the period since the data assimilation remains the same over 1871–2010.

The winter seasons of the 1901–2010 period are categorized into two groups corresponding to the AMO+ and
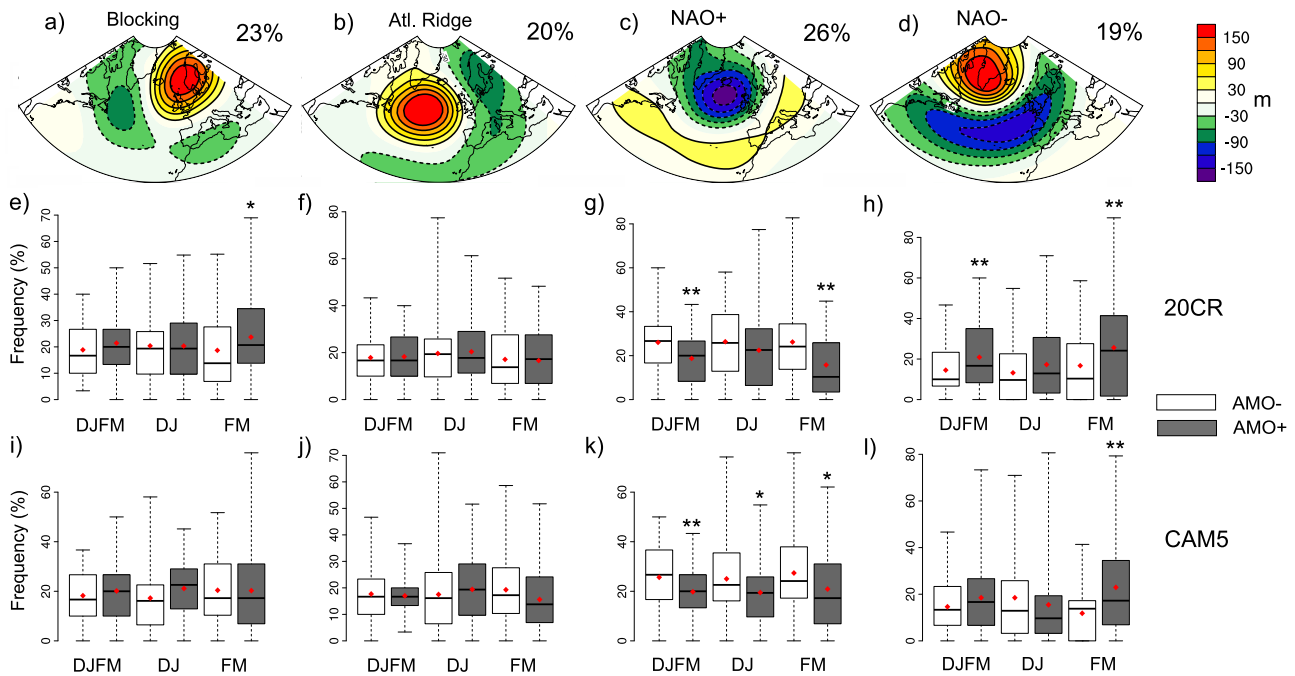
Figure 3. Response of the North Atlantic intraseasonal weather regimes to the AMO. (a)–(d) Winter (DJFM) North Atlantic weather regimes computed over 1901–2010 from the Z500 anomalies (in m) of 20CR. Frequencies of occurrence over the 1901–2010 wintertime days are indicated in %. (e)–(h) Distribution of seasonal regime frequencies in 20CR over 1901–2010, during AMO− (53 years, white boxplots) and AMO+ (57 years, gray boxplots) for winter (DJFM), early (DJ) and late (FM) winter. (i)–(l) same as (e)–(h) except for CAM5 (AMOn in white and AMOp in gray, 50 years for each experiment). Boxplots indicate the maximum, upper-quartile, median, lower-quartile and minimum of the distribution (horizontal bars). The mean of the distribution is shown by red diamonds, and asterisks indicate the significance level of the difference of the mean between AMO− and AMO+ (AMOn and AMOp for the simulations): *: $p < 0.1$; **: $p < 0.05$ (t-test).

AMO− years (same years as in figure 2(a)). The mean and the distribution of the seasonal frequencies for each regime and the AMO polarity are shown in figures 3(e)–(h) for the entire (DJFM), early (DJ) and late (FM) winter. The more significant changes are found for the NAO− and NAO+ regimes (figures 3(g) and (h)), in line with the NAO pattern identified in figure 2(a). When the AMO is positive, the frequency of the NAO+ regime is decreased, while the frequency of the NAO− regime is increased. This result is significant according to a student t-test applied to the mean of the frequencies. It is found both in early and late winter and is stronger and statistically significant in February–March. The distribution shifts towards lower (higher) values for the NAO+ (NAO−) regimes during the AMO+ compared to the AMO−. In particular, extreme values of the NAO− frequency are larger during AMO+ (figure 3(h)), suggesting that extreme cold winters over Europe that occur with a persistent negative NAO regime (like in 2009–2010 Cattiaux *et al* 2010) are more probable during the positive phase of the AMO. The increase in frequency of the blocking regime during the AMO+ (figure 3(e)) is consistent with the results of Häkkinen *et al* (2011) and also favorable to cold extreme conditions over Europe.

3.3. Additional evidence using numerical simulations

The observational results highlight a statistical relationship between the AMO and the decadal fluctuations of the atmospheric circulation, but it is hard to attribute causality. The

AMO may force the NAO and the change in the frequency distribution of the weather regimes, but it also responds to the persistence of these atmospheric anomalies (Li *et al* 2013, Eden and Jung 2001). Still the lead–lag correlations of figure 2(b) suggest that the AMO precedes the NAO. The causal relationship is further examined by using an atmospheric GCM to simulate the response of the atmosphere to AMO forcing. The weather regimes analysis is applied to the daily outputs of the AMOp and AMOn simulations (see section 2 for a description of the experiments). The model represents the four major weather regimes identified in 20CR with realism and also captures their impact on surface temperature (figure S5 available at stacks.iop.org/ERL/9/0340 18/mmedia). The respective distribution of the frequencies of each regime is shown in figures 3(i)–(l). There is a remarkable agreement between 20CR and CAM5 concerning the impact of the AMO on the frequencies of the weather regimes. The frequency of the NAO+ regime is decreased while the frequencies of the NAO− and blocking regimes are increased, especially in late winter. The seasonal mean of the SLP response also resembles the NAO pattern with larger amplitude in late winter (figure S6(c) available at stac ks.iop.org/ERL/9/034018/mmedia), in line with 20CR. These modeling results support the idea that the AMO is actually causing the atmospheric anomalies identified in observations. The current positive phase of the AMO has therefore promoted the occurrence of negative NAO anomalies and more frequent blocking conditions during the last winters. In line with the
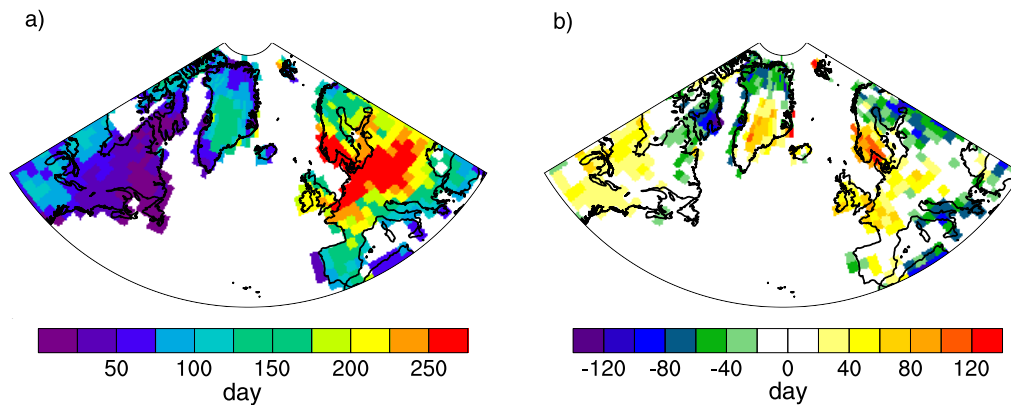
a)

b)

Figure 4. Impact of the AMO on the occurrence of cold spells. (a) Cumulative number of cold spell days in AMOp (50 winters). (b) Response to the AMO forcing (AMOp–AMOn) in number of cold spell days.

dynamical response to the AMO, extreme cold temperatures were observed over Europe and eastern North America. This thermodynamical response is also captured by our model since the number of winter cold spell days increases in AMOp compared to AMOn in northern/western Europe and in the eastern US (figure 4).

In figure 5 we examine the physical mechanism that may explain the dynamical response to the AMO. The positive phase of the AMO, compared with the negative phase, induces an equatorward shift of the transient eddy activity (standard deviation of the 500 hPa geopotential height) in winter both in observations (figure 5(a)) and CAM5 (figure 5(b)). The decrease in the transient eddy activity around 45°N is consistent with the negative NAO response to the positive AMO. Indeed, the eddy activity is modulated by the zonal mean flow anomalies but is also critical for maintaining the westerly winds associated with the positive NAO (Hoskins *et al* 1983). The response in transient eddy activity is mainly driven by changes in the SST field in the region of the Gulf Stream, off the coast of Newfoundland. The Atlantic storm track emerges in this region of strong land–sea thermal contrast and high baroclinicity in the atmosphere (Brayshaw *et al* 2011). The SST anomalies associated with the AMO are at maximum in this region (figure 1(b)). During the positive AMO, the warm SST anomaly reduces the meridional SST gradient (figure S7(a) available at stacks.iop.org/ERL/9/034018/mmedia) and energy is released to the atmosphere through latent heat flux anomalies (figure 5(c)). The vertical profile of temperature is perturbed in the troposphere (figure S7(b) available at stacks.iop.org/ERL/9/034018/mmedia) and the area of maximum baroclinicity is shifted southward as illustrated in figure 5(d) by the anomalies in the Eady growth rate (zonally averaged over the west North Atlantic sector). This physical mechanism involving a change in the baroclinicity and a shift in the transient eddy activity is in agreement with a previous GCM study (Msadek *et al* 2011).

4. Discussion and conclusion

Our results highlight the potential predictability at the decadal time scale that is associated with the AMO for predicting

winter climate for the North Atlantic sector and adjacent continents. Unlike the recent study of Li *et al* (2013), we find that at the multidecadal time scale, the AMO–NAO relationship is stronger when the AMO leads the NAO. Nevertheless, it does not rule out that the NAO in turn exerts a forcing on the AMOC and the North Atlantic SSTs (Eden and Jung 2001, Mecking *et al* 2013). This two-way interaction should be investigated further in future studies using coupled ocean–atmosphere models. Both observational evidence and modeling results suggest that the positive phase of the AMO induces anomalies of the atmospheric circulation that promote episodes of cold temperature over Europe and eastern US in winter. It is therefore quite plausible that the resurgence of severe winter weather over these regions is promoted by the current positive polarity of the AMO. Not taking this factor into account may lead to overestimation of the role of the Arctic amplification phenomenon, which is another potential driver (Francis and Vavrus 2012). Since a part of the recent Arctic sea ice loss is attributable to the influence of the AMO (Day *et al* 2012), the AMO may also have an indirect effect on the atmospheric circulation through sea ice anomalies of the Arctic region. This effect is secondary in our experiments in which the sea ice anomalies are small and are prescribed over the North Atlantic only. In nature the sea ice anomalies are greater both in spatial extent and amplitude since the anthropogenic signal is superimposed on the natural variability. Provided that the AMO remains in its positive polarity for one to two additional decades, cold and snowy weather conditions in winter should be favored over Europe and the eastern US. Nevertheless, the near-term evolution of the AMO is uncertain and other factors may modulate the impact of the AMO on North Atlantic variability (e.g. Arctic sea ice loss, Pacific Decadal Oscillation, solar forcing, volcanic eruptions, etc). The anthropogenic signal-to-noise ratio is also expected to increase in coming decades while the greenhouse gas concentrations continue to increase in the atmosphere (IPCC 2007), adding uncertainty to the future of wintertime cold extremes in mid-latitude continental areas of the Northern Hemisphere.
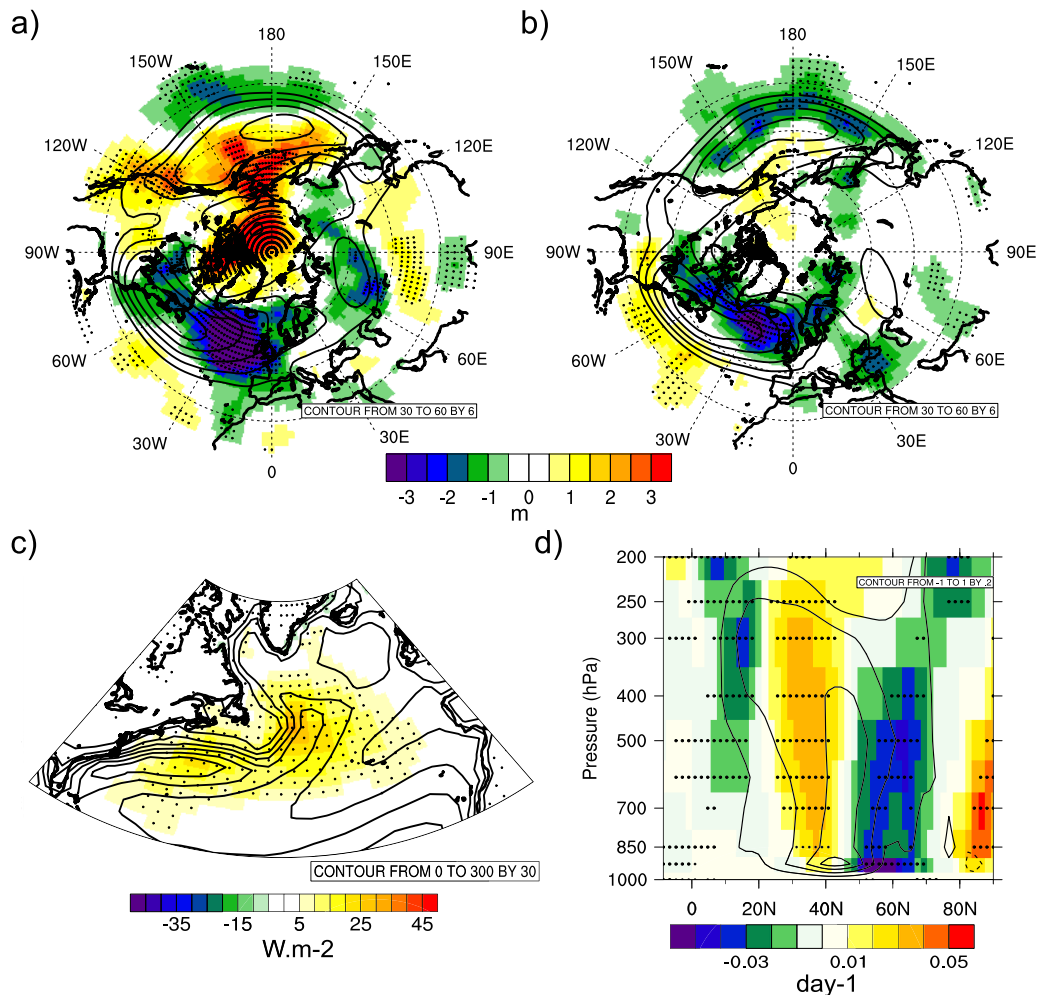
Figure 5. Physical mechanism of the atmospheric response to the AMO. (a) Winter (DJFM) transient eddy activity anomalies at 500 hPa associated with the AMO signal (57 AMO+ years minus 53 AMO− years, see list in text) in 20CR over 1901–2010 (shading in m). The climatology of transient eddy activity is shown in contours. (b) Same as (a) except for CAM5 (AMOp minus AMOn). (c) DJFM anomalies of the surface latent heat flux (shading, W m^{-2}) in CAM5 (AMOp–AMOn) and climatology in contours. (d) Pressure versus latitude plot of the DJFM Eady growth rate anomalies (day-1) over western North Atlantic (75W/30W) in CAM5 (AMOp–AMOn) and climatology in contours. Anomalies significant at the 95% level are stippled.

Acknowledgments

References

Barnes E A 2013 Revisiting the evidence linking Arctic amplification to extreme weather in midlatitudes *Geophys. Res. Lett.* **40** 4728–33

Booth B B B, Dunstone N J, Halloran P R, Andrews T and Bellouin N 2012 Aerosols implicated as a prime driver of twentieth-century North Atlantic climate variability *Nature* **434** 228–32

Brayshaw D J, Hoskins B and Blackburn M 2011 The basic ingredients of the North Atlantic storm track. Part II: sea surface temperatures *J. Atmos. Sci.* **68** 1784–805

Cassou C 2008 Intraseasonal interaction between the Madden–Julian Oscillation and the North Atlantic Oscillation *Nature* **455** 523–7

Cattiaux J, Vautard R, Cassou C, Yiou P, Masson-Delmotte V and Codron F 2010 Winter 2010 in Europe: a cold extreme in a warming climate *Geophys. Res. Lett.* **37** L20704

Cohen J L, Furtado J C, Barlow M A, Alexeev V A and Cherry J E 2012 Arctic warming, increasing snow cover and widespread boreal winter cooling *Environ. Res. Lett.* **7** 014007

Compo G P *et al* 2011 The twentieth century reanalysis project *Q. J. Geol. Meteorol. Soc.* **137** 1–28

Coumou D and Rahmstorf S 2012 A decade of weather extremes *Nature Clim. Change* **2** 491–6

Day J J, Hargreaves J C, Annan J D and Abe-Ouchi A 2012 Sources of multi-decadal variability in Arctic sea ice extent *Environ. Res. Lett.* **7** 034011

Dima M and Lohmann G 2007 A hemispheric mechanism for the Atlantic Multidecadal Oscillation *J. Clim.* **20** 2706–19

Eden C and Jung T 2001 North Atlantic interdecadal variability: oceanic response to the North Atlantic Oscillation (1865–1997) *J. Clim.* **14** 676–91

Francis J and Vavrus S 2012 Evidence linking Arctic amplification to extreme weather in mid-latitudes *Geophys. Res. Lett.* **39** L06801

Gastineau G, D'Andrea F and Frankignoul C 2013 Atmospheric response to the North Atlantic Ocean variability on seasonal to decadal time scales *Clim. Dyn.* **40** 2311–30

Häkkinen S, Rhines P B and Worthen D L 2011 Atmospheric blocking and Atlantic Multidecadal Ocean variability *Science* **334** 655–9

Hoskins B J, James I N and White G H 1983 The shape, propagation and mean-flow interaction of large-scale weather systems *J. Atmos. Sci.* **40** 1595–612

Hurrell J W, Kushnir Y, Ottersen G and Visbeck M 2003 *The North Atlantic Oscillation: Climate Significance and Environmental Impact (Geophysical Monograph Series* vol 134*)* p 279

IPCC 2007 Climate change 2007: the physical science basis *Contribution of Working Group I to the Fourth Assessment Report of the IPCC* ed S Solomon, D Qin, M Manning, Z Chen, M Marquis, K B Averyt, M Tignor and H L Miller (Cambridge: Cambridge University Press) p 996

Kavvada A, Ruiz-Barradas A and Nigam S 2013 AMO's structure and climate footprint in observations and IPCC AR5 climate simulations *Clim. Dyn.* **41** 1345–64

Kerr R A 2000 A North Atlantic climate pacemaker for the centuries *Science* **288** 1984–6

Knight J R, Folland C K and Scaife A A 2006 Climate impacts of the Atlantic Multidecadal Oscillation *Geophys. Res. Lett.* **33** L17706

Knudsen M F, Seidenkrantz M S, Jacobsen B H and Kuijpers A 2011 Tracking the Atlantic Multidecadal Oscillation through the last 8000 years *Nature Commun.* **2** 1–8

Li J, Sun C and Jin F-F 2013 NAO implicated as a predictor of Northern Hemisphere mean temperature multidecadal variability *Geophys. Res. Lett.* **40** 5497–502

Mahajan S, Zhang R and Delworth T L 2011 Impact of the Atlantic Meridional Overturning Circulation (AMOC) on Arctic surface air temperature and sea ice variability *J. Clim.* **24** 6573–81

Mecking J V, Keenlyside N S and Greatbatch R J 2013 Stochastically-forced multidecadal variability in the North Atlantic: a model study *Clim. Dyn.* doi:10.1007/s00382-013-1930-6

Msadek R, Frankignoul C and Li L 2011 Mechanisms of the atmospheric response to North Atlantic multidecadal variability: a model study *Clim. Dyn.* **36** 1255–76

Ouzeau G, Cattiaux J, Douville H, Ribes A and Saint-Martin D 2011 European cold winter 2009–2010: how unusual in the instrumental record and how reproducible in the ARPEGE-climat model? *Geophys. Res. Lett.* **38** L11706

Peings Y and Magnusdottir G 2014 Response of the wintertime Northern Hemisphere atmospheric circulation to current and projected Arctic sea ice decline: a numerical study with CAM5 *J. Clim.* **27** 244–64

Rayner N A, Parker D E, Horton E B, Folland C K, Alexander L V, Rowell D P, Kent E C and Kaplan A 2003 Global analyses of sea surface temperature, sea ice, and night marine air temperature since the late nineteenth century *J. Geophys. Res.* **108** 4407

Screen J A and Simmonds I 2010 The central role of diminishing sea ice in recent Arctic temperature amplification *Nature* **464** 1334–7

Screen J A and Simmonds I 2013 Exploring links between Arctic amplification and mid-latitude weather *Geophys. Res. Lett.* **40** 959–64

Stroeve J C, Kattsov V, Barrett A, Serreze M, Pavlova T, Holland M and Meier W N 2012 Trends in Arctic sea ice extent from CMIP5, CMIP3 and observations *Geophys. Res. Lett.* **39** L16502

Tang Q, Zhang X, Yang X and Francis J A 2013 Cold winter extremes in northern continents linked to Arctic sea ice loss *Environ. Res. Lett.* **8** 014036

Trenberth K E and Shea D J 2006 Atlantic hurricanes and natural variability in 2005 *Geophys. Res. Lett.* **33** L12704

Walsh J E and Chapman W L 2001 20th-century sea-ice variations from observational data *Ann. Glaciol.* **33** 444–8

Wang C and Zhang L 2013 Multidecadal ocean temperature and salinity variability in the tropical North Atlantic: linking with the AMO, AMOC, and subtropical cell *J. Clim.* **26** 6137–62

Yiou P and Nogaj M 2004 Extreme climatic events and weather regimes over the North Atlantic: when and where? *Geophys. Res. Lett.* **31** L07202